



DYNAMIC BEHAVIOUR STUDY OF ALL-TERRAIN VEHICLE DRIVETRAIN

Ion Preda¹, Gheorghe Ciolan²

¹ Transilvania University, Brasov, ROMANIA, e-mail: pion@unitbv.ro

² Transilvania University, Brasov, ROMANIA, e-mail: cgicu@unitbv.ro

Abstract:

The paper presents a theoretical method used to determine transmission strain peaks and also some aspects concerning the dynamic behaviour of an experimental all-terrain vehicle. The results of computer aided simulation are compared with experimental measurements to validate the dynamic and mathematical models.

Keywords:

all terrain vehicle, drivetrain, dynamic behaviour, simulation, experiment

1. INTRODUCTION

Given their high values, the mechanic strains generated during drivetrain couplings influence decisively the service life and the general behaviour of motor vehicle propulsion equipment. Further, the torque values attained in these situations represent the starting point for most dimensional calculations of drivetrain components.

2. CLUTCH MODELLING

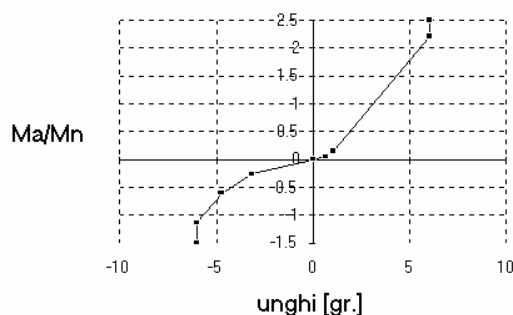


Figure 1: Theoretical elastic characteristic of the clutch vibration damper (Ma/Mn vs. angle)

By its operation mode and depending on the working parameters, the clutch can represent a strong damping element for the transmission, but also a disturbing one.

An element difficult to model is the vibration damper, placed between the friction disk and its hub, one of its purposes being the drivetrain strain diminishing in case of shock. The characteristic of the studied clutch elastic element is non-linear, consisting of three parts of different rigidities, for each torsion way, **figure 1**. The damping element operates by dry friction and contributes to the amplitude diminishing of torsion oscillations. The hysteresis generated by this is about $\pm 10\%$ of the engine rated torque M_n , as can be seen in **figure 2**.

In order to study the strain in the transmission generated at starting or gear shifting, also the capable torque of the clutch has to be known. This is given by the equation:

$$M_a = i \mu F R_{med} \quad (1)$$

where i represents the number of friction surfaces (in the considered case $i=2$); μ – the friction coefficient; F – the clamping force of the friction disk; R_{med} – the average radius of the friction set.

Figure 3 presents the case of the analysed diaphragm-spring clutch. The friction-disk clamping-force F depends on the pressure-plate axial displacement f with respect to the flywheel (the reference position being the one in which the distance from the pressure disk to the flywheel is equal to the non-compressed thickness of the friction disk). A second dependence can be noticed between the stroke c of the throwout bearing and its displacement f .

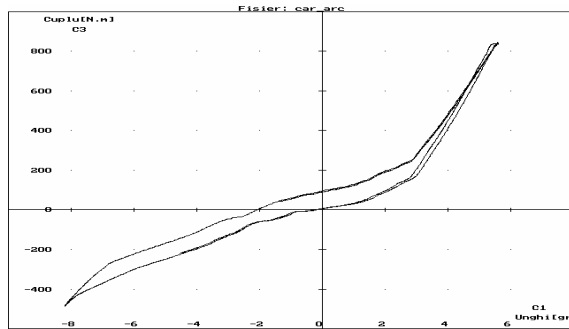


Figure 2: Experimental elastic characteristic of the clutch vibration-damper

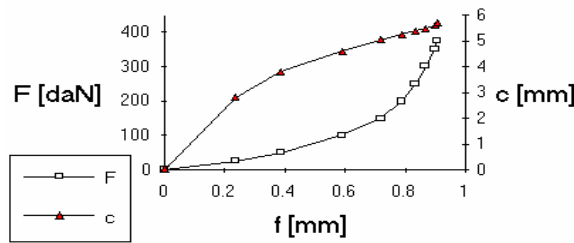


Figure 3: Axial deformation characteristic of the friction disk; throwout bearing displacement vs. pressure disk displacement

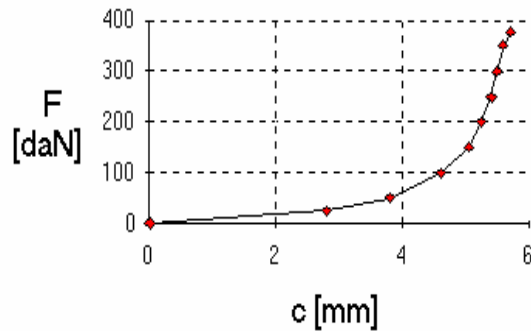


Figure 4: Friction-disk clamping force vs. throwout-bearing stroke

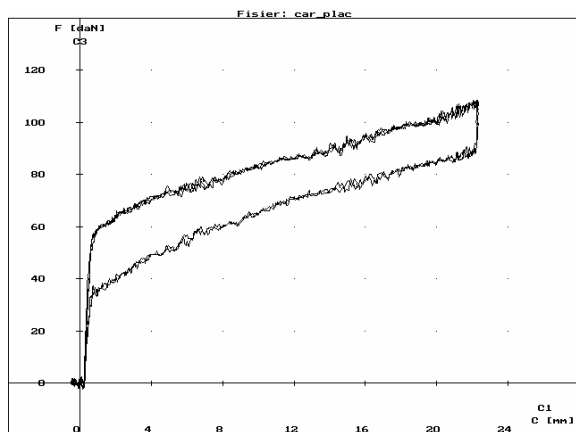


Figure 5: Actuation force vs. stroke for the throwout bearing

Based on these characteristics, **figure 4** shows the experimentally established function between the force F and the stroke c , representing the connection between the driver action (position of the clutch pedal p_a) and the capable clutch torque (the value for that slip occurs). By permanent comparison of this value with the elastic moment, the developed algorithm will point out the eventual slip of the clutch (including short slip durations after the release of the clutch pedal, consequently to the overloads that may occur in the drivetrain).

Experiments conducted on the test bench have emphasized that in actuating the diaphragm spring clutch a significant hysteresis is generated, **figure 5**, that has to be taken into consideration in both simulation of driving actions and clutch automation.

MODELLING OF GEARBOX AND TRANSFER BOX

The extended dynamic model used for the experimental vehicle gearbox is presented in **figure 6**. It includes three shafts (the primary shaft, the secondary shaft and the driven shaft of the bevel gear) and the gear wheels (a total of 17 flywheels). The lines between the flywheels represent rigidities, the continuous ones being permanent links, while the dashed ones become active only when the respective gear is coupled. The small squares attached to some of the flywheels represent transmission ratios. The model is quite complex, but allows a detailed analysis of the gearbox operation, considering also the damping (frictions in gears, in bearings or between wheels and oil) for the study of transitory and stabilised operation modes, as well as vibration frequency analysis.

The flywheels represented in figure 6 correspond to the following components: 1 – friction disk of the clutch; 2 – clutch hub; 3, 4, 5, 6, 7 – driving wheels of gears I, II, III, MI (reverse) and IV; 8, 9, 10, 12 – driven wheels of gears I...IV; 11 – intermediate backward wheel; 13 – driven backward wheel and synchronesh III-IV; 14 – synchronesh I-II; 15 – bevel driving gear; 16 – driven bevel gear; 17 – coupling flange and half of the cardan between gearbox and transfer box.

However, a model of this complexity may be unjustified for the study of the general behaviour of the drivetrain. Still, based on this complex model, the masses and elastic constants can be reduced accurately, and the location of the equivalent inertia moment can be established. In the analysed case, the reduction was carried out in relation to the secondary shaft of the gearbox, mid-placed in relation to the flywheels' totality. Under these circumstances, the equivalent inertia moment, determined based on the conservation of kinetic energy, will change for each coupled gear, in accordance with the following equation:

$$J_{ech} = \sum_m J_m \cdot i_m^2 \quad (2)$$

where J_m represents the inertia moment in relation to the rotation axis of a certain flywheel m , and i_m is the transmission ratio from the flywheel m to the element in relation to which the reduction is conducted.

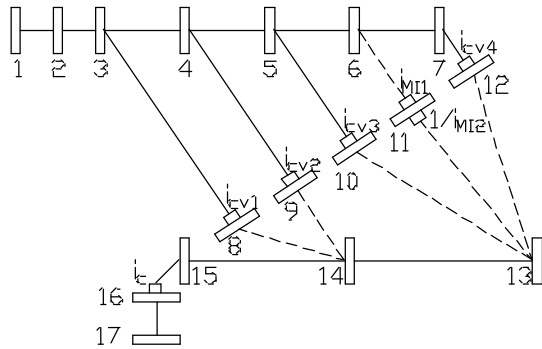


Figure 6: Extended dynamic model of the gearbox

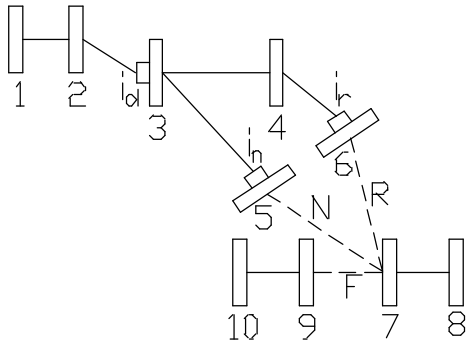


Figure 7: Extended dynamic model of the transfer box

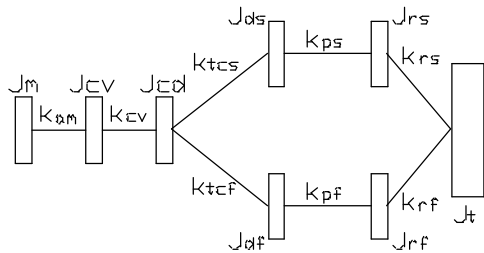


Figure 8: General model of the drivetrain (without inter-axial differential)

oscillations and torsional strains, respectively.

DRIVETRAIN GENERAL MODEL OF THE ANALYSED OFF-ROAD VEHICLE

Modelling of the general drivetrain was realized based on the principles of modularity, so that changing of the employed diagram should not raise special problems in the development of the simulation programmes. The main aim was the development of a drivetrain without an inter-axial (centre) differential. Starting from here, the model with eight flywheels presented in **figure 8** was achieved.

The inertia moments and the stiffness and damping constants were obtained by reducing the extended models of the subassemblies presented previously. The indices used for the individualisation of the inertia moments had the following significance: *m* - engine; *cv* - gearbox; *cd* - transfer box; *d* - differential; *r* - wheel; *f* - front; *s* - rear. Considering equivalent kinetic energy, for the mass in linear motion an equivalent inertia moment was used, determined by the following relation:

$$J_t = m \cdot r_d^2, \quad (4)$$

where *m* and *r_d* represent the total mass of the vehicle and the dynamic radius of the wheel, respectively. Further the relative motions on the displacement direction between the unsprung- and the sprung masses were neglected. As can be noticed, the four branches of the transmission between the axle differentials and wheels were reduced to only two: one for the front and one for the rear axle. This was achieved in order to simplify the model such as to facilitate its solving, based on the assumption of identical strains on the wheels of the same axle.

The reduction of the elastic torsion constants is achieved by considering the elastic elements connected in series,

$$k_{ech} = \frac{1}{\sum_n \frac{1}{k_n}}, \quad (3)$$

k_n representing the torsional rigidity of a segment between two neighbouring flywheels.

As operational principle, the synchronisers are quite similar to clutches, but their friction surfaces (usually conical) function in oil. The tests revealed that during the synchronisation process a constant value can be assumed for the friction coefficient ($\mu=0.1$), excepting a short time interval, when the oil is eliminated from between the surfaces in friction. Thus equation (1) can be applied also for the synchronisation moment *M_s* that can be assumed as directly proportional with the actuating force *F*.

Figure 7 presents the extended dynamic model of the transfer box, achieved similarly to that of the gearbox. It includes four shafts, each having two flywheels to which the two free wheels placed on the secondary shaft are added. The links denoted with *N*, *R* and *F* are achieved respectively when selecting the range of normal speeds, when selecting the range of reduced speeds or when coupling the front axle (*N* and *R* exclude each other).

The flywheels correspond respectively to: 1 - the input flange plus half of the cardan between the gearbox and the transfer box; 2 - the driving gear plus the input shaft; 3 - the intermediate gear for the normal range plus half of the intermediate shaft; 4 - the intermediate wheel for the reduced shaft plus half of the intermediate shaft; 5, 6 - driven gears for the normal and the reduced range; 7 - normal/reduced coupling element; 8 - output flange towards the rear axle plus half of the first rear cardan shaft; 9 - coupling element of the front axle; 10 - output flange towards the front axle plus half of the front cardan. The values of rigidities and inertia moments were computed and then verified in part by measurements as pendulum

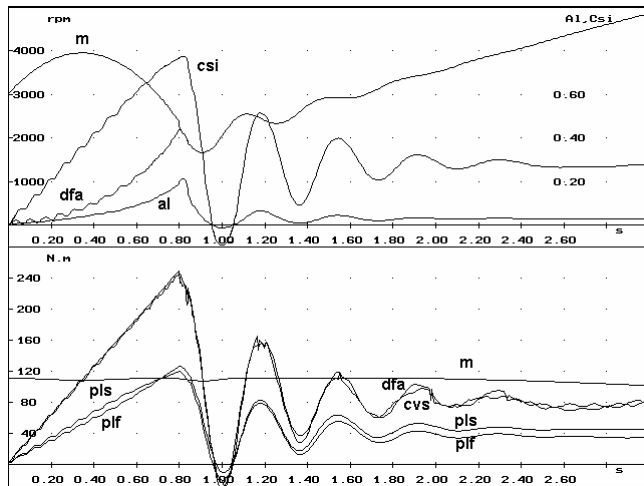


Figure 9: Starting from the spot, 1st gear, 4x4N, $\mu=0.8$, $t_c=1$ s, $n=3000$ rpm (computed values)

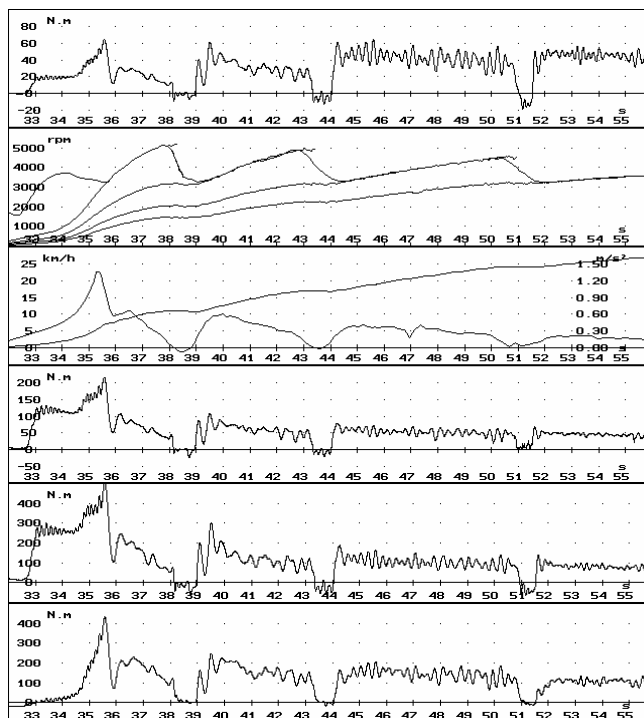


Figure 10: Starting from the spot, gears I...IV, 4x4R, dry asphalt (measured values)

does not exceed 20%. Also, the high rigidity of the transmission and implicitly its increased capacity of accumulating elastic deformation energy determine a significant relaxation of the transmission, the torques becoming negative immediately after the clutch engagement. It is also for this reason that the vibrations' decoupling is not sufficient at the clutch damper and the engine speed oscillates.

The clutch is intensely strained, the maximum torque transmitted by it exceeding about 2.2 times the effective torque of the engine, compared to 1.4 times achieved for the case of rear wheel drive. It can be further noticed that, during the final period of clutch coupling, the torque at the front axle shafts exceed that of the rear ones. This apparently strange phenomenon, observed experimentally too, **figure 10**, can be explained by the strong pitching that, modifying the normal loads on the two axles, increase the dynamic radii of the front wheels and decrease those of the rear ones. Thus, by the greater slipping of the front wheels, the effect of the specific tangential force growth exceeds that of the rated load decrease.

Another aspect worth highlighting is the strong damping of oscillations due mostly to the sliding of the wheels on the road surface. During the sliding of the driving wheels, the occurrence of torsional vibrations can be noticed, started already in the clutch slipping phase, showed by speed variations particularly at wheel level. The frequencies of the mentioned oscillations correspond to the first two vibration natural shapes and natural frequencies of the drivetrain: 1.6 Hz and 19.7 Hz.

The dynamic model of **figure 8** corresponds exactly to the situation of 4WD. For rear wheel drive, the ideal shaft between J_{rf} and J_t must be removed (in the computer programme, null value assumes for the rigidity k_{rf}).

It was considered that the mechanic system is subjected to external moments (the effective engine torque and the global resistance torque), as well as to drivetrain internal moments (friction moments between clutch and synchronisers). For the clutch and wheels only damping due to dry friction was considered. For the subassemblies with gears operating in oil the authors have employed damping moments include, additionally to the component proportional to the rotation speed, a component proportional to the square of the rotation speed. This is justified by the fact that the gears operate as hydraulic pumps. As for the engine, this was assessed generally by the effective torque, depending upon two parameters: speed and position of the acceleration pedal.

STARTING FROM REST

For a convenient interpretation of the qualitative and quantitative aspects, computation results were represented graphically. The upper part of the graphs represents the curves of the speeds reduced to the engine crankshaft, the sliding, *al*, and the specific tangential forces on the driving wheels, *csi*, while the lower part shows the time related evolution of torques.

The used symbols are: *m* – engine; *dfa* – friction disk of clutch; *cvs* – secondary shaft of gearbox; *rs* – rear wheel; *plf*, *pls* – front- and rear axle shaft.

Figure 9 shows the results of starting from the spot in 4WD case. The figure corresponds to acceleration on a good-friction level road ($\mu=0.8$), in the first gear. It was considered a constant speed release of the clutch pedal, in one second ($t_c=1$ s) and starting at the moment $t=0$. Further, the engine operates on its full-throttle characteristic.

Due to the 4WD, it could be noted that the sliding

Monitoring the time related evolution of the engine angular speed, it can be noticed that this is insignificantly influenced by the oscillations generated in the transmission (this aspect becomes even more evident for the case of rear wheel drive). This proves that the clutch damper correctly fulfils its role of decoupling transmission and engine vibrations.

The brief description of the vehicle propulsion equipment behaviour was given in order to prove the manner in which simulation can contribute to the assessment and use of experimental results, that sometimes are not sufficient themselves to determine cause and nature of the observed phenomena.

Thus **figure 10** presents the recording of a starting process, for road conditions similar to those described above, but using the slow range (gear) of the transfer box.

The quantities of the six zones of the graph, upwards, represent respectively: M_f – front planetary gear torque; M_s – rear planetary gear torque; M_t – rear cardan torque; v – vehicle velocity and a – vehicle acceleration; nm – engine speed and nt – rear cardan speed, the latter one reduced to the clutch friction disk; M_{fa} – torque transmitted by the clutch, deduced from the torques of the front and rear axle shafts, assuming that the shafts of the same axle are strained identically.

GEAR SHIFT

Significant strain of the transmission occurs during gears' shifting or changing "by driving" from rear wheel drive to all-wheel drive. Both situations were studied by the help of the simulation programme.

Figure 11 shows shifting from first to second gear, the transfer box ensuring 4WD and range ratio for normal running condition (4x4N). It was selected an friction coefficient $\mu=0.5$ (corresponding to dry soft ground) and an clutch pedal releasing interval of 1.8 s.

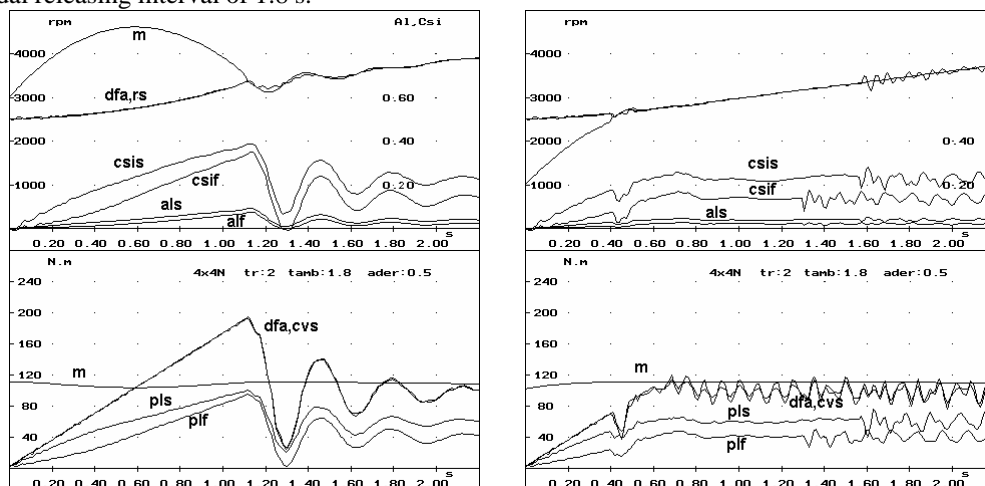


Figure 11: Shift from first to second gear, 4x4N, $\phi=0.5$, $t_c=1.8$ s, $n=3000$ rpm (left) and $n=1000$ rpm (right)

The difference between the situation presented in the figure above lies in the initial values of the speed from the starting moment of the clutching process (3000 rpm and 1000 rpm). In the first case (left), the engine, full throttled and having a speed already higher than that of the clutch friction plate, will race to approximately 4500 rpm, after that it has to reduce its speed, being intensively braked by the transmission.

The kinetic energy accumulated by the engine in the first phase of the clutch coupling is released to the drive wheels, contributing to a more intensive acceleration and increasing significantly the strain in the transmission. The torque transmitted by the clutch exceeds the engine rated torque by about 75% and the sliding of the clutch lasts 1.1 s.

In the second case (right), the release of the acceleration pedal in order to engage the second gear, contributes substantially to the decrease of the mechanical (and thermal) strains on the clutch: the clutch torque will not exceed the engine one anymore, while the clutch sliding takes only 0.4 s.

It is interesting to note that the relaxation phenomenon of the transmission following equalisation of engine and clutch disk speeds will now be much less intensive and will initiate much weaker oscillations.

A rather frequently used manoeuvre in all terrain vehicles with optionally coupled front axle consists in its coupling during running. This proves extremely useful particularly during races, when running takes place at the limit of friction. Due to large tangential forces, in turns the lateral controllability of the rear wheels can be diminished. At the moment when the pronounced oversteering behaviour of the vehicle becomes undesirable, the front axle will be coupled. Due to its contribution to the traction process, the slipping of the rear wheels will be reduced, as shown in **figure 12**. Gradually the vehicle will reach a neutral attitude, what can lessen the consequences of a critical situation.

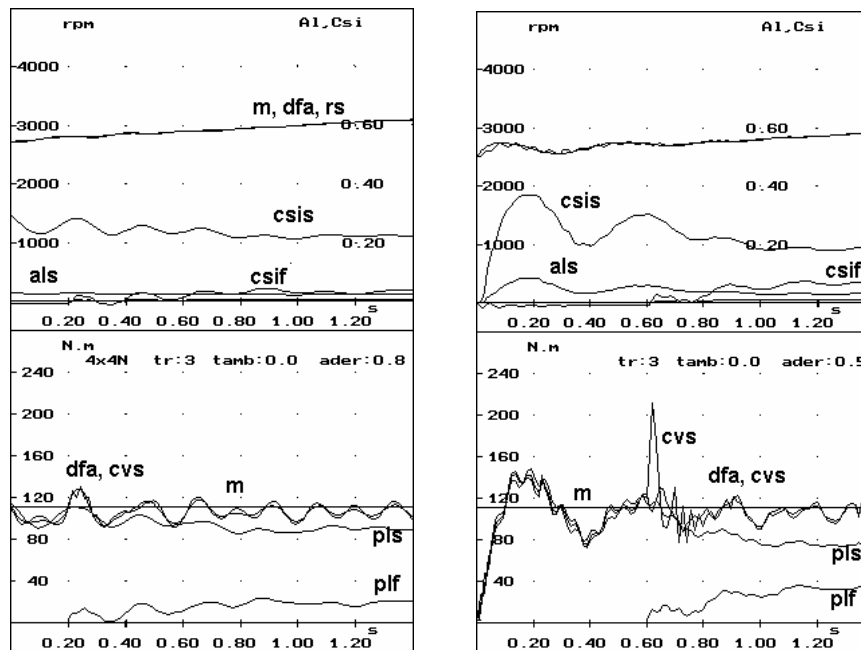


Figure 12: Coupling during running of the front axle, asphalt (left) and dry earth (right)

As for the shocks generated by the front axle coupling during running these are felt more acutely in the area of the transfer box and are more intensive for greater values of the rear axle slipping, **figure 12, right**.

CONCLUSIONS

The comparison of the theoretical and experimental results has yielded a good concordance, mostly from the qualitative viewpoint. Similar evolutions can be stated, both for the angular velocities and the torques. The differences that occur are due firstly to the more intensive damping in the case of the measured strain and to the longer releasing time of the clutch pedal in the real situation, opposed to the simulated one.

The obtained results show that the employed theoretical model allows for simulation of processes difficult to study experimentally. Further, an accurate dimensioning of the transmission subassemblies becomes possible already in the design phase.

REFERENCES

- [1] Câmpian, V. Vulpe, V. Ciolan, Gh. Enache, V. Preda, I. Câmpian, O.: *Automobile* (Motor vehicles). University of Brasov, 1989.
- [2] Ciolan, Gh. Preda, I.: *Study of cross-country car transmission strains*. International Congress "MOTAUTO '97", volume II, p.49-54, Russe, 1997.
- [3] Ciolan, Gh. Preda, I. Peres, Gh. *Cutii de viteze pentru automobile* (Automotive transmissions). Editura Didactica si Pedagogica, Bucuresti, 1998.
- [4] Ciolan, Gh.: *Studiul solicitarilor din transmisia autoturismelor de teren tip Aro, în vederea optimizarii constructiilor* (Study of strains in all-terrain motor-vehicle drivetrain). Ph.D. dissertation, University of Brasov, 1991.
- [5] Mitsche, M.: *Dynamik der Kraftfahrzeuge* (Motor vehicle dynamics). Springer Verlag, New York, 2004.
- [6] Preda, I.: *Studiul solicitarilor din transmisia autoturismelor de teren, în vederea optimizarii acesteia*. (Study of strains in all-terrain motor-vehicle drivetrain for their optimisation.) Ph.D. dissertation, University of Brasov, 1993.
- [7] Preda, I. Ciolan, Gh. Dogariu, M. Todor, I. Computer model to simulate the vehicle longitudinal dynamics. In: Bulletin of the Xth International Conference CONAT, paper 1060, Brasov, 2004.
- [8] Untaru, M. Potincu, Gh. Stoicescu, A. Peres, Gh. Tabacu, I. *Dinamica autovehiculelor pe roti* (Dynamics of wheeled vehicles). Editura Didactica si Pedagogica, Bucuresti, 1981.